L-type Ca v 1.3 channels regulate ryanodine receptor-dependent Ca 2+ release during sino-atrial node pacemaker activity

Angelo Torrente, Pietro Mesirca, Patricia Neco, Riccardo Rizzetto, Stefan Dübel, Christian Barrère, Martina Sinegger-Brauns, Joerg Striessnig, Sylvain Richard, Joël Nargeot, et al.

HAL Id: hal-01792471

https://hal.umontpellier.fr/hal-01792471

Submitted on 28 Mar 2020

L-type $Ca_v1.3$ channels regulate ryanodine receptor-dependent Ca^{2+} release during sino-atrial node pacemaker activity

Angelo Giovanni Torrente[1,2,3†*], Pietro Mesirca[1,2,3‡], Patricia Neco[4,5‡], Riccardo Rizzetto[1,2,3], Stefan Dubel[1,2,3], Christian Barrere[1,2,3], Martina Sinegger-Brauns[5,6], Joerg Striessnig[5,6], Sylvain Richard[7,8], Joël Nargeot[1,2,3], Ana Maria Gomez[4,5], and Matteo Elia Mangoni[1,2,3*]

[1]Département de Physiologie, CNRS, UMR-5203, Institut de Génomique Fonctionnelle, Montpellier F-34000, France; [2]INSERM, U1191, Montpellier F-34000, France; [3]Université de Montpellier, UMR-5203, Montpellier F-34000, France; [4]UMR-S 1180, Inserm, Univ. Paris-Sud, Université Paris-Saclay, Châtenay-Malabry, France; [5]Department of Pharmacology and Toxicology, Institute of Pharmacy; [6]Center for Molecular Biosciences, University of Innsbruck, Innsbruck, Austria; [7]INSERM, U1046, Montpellier, France; and [8]CNRS UMR 9214, PhyMedExp, University of Montpellier, France

Aims	Sino-atrial node (SAN) automaticity is an essential mechanism of heart rate generation that is still not completely understood. Recent studies highlighted the importance of intracellular Ca^{2+} ($[Ca^{2+}]_i$) dynamics during SAN pacemaker activity. Nevertheless, the functional role of voltage-dependent L-type Ca^{2+} channels in controlling SAN $[Ca^{2+}]_i$ release is largely unexplored. Since $Ca_v1.3$ is the predominant L-type Ca^{2+} channel isoform in SAN cells, we studied $[Ca^{2+}]_i$ dynamics in isolated cells and *ex vivo* SAN preparations explanted from wild-type (WT) and $Ca_v1.3$ knockout (KO) mice ($Ca_v1.3^{-/-}$).
Methods and results	We found that $Ca_v1.3$ deficiency strongly impaired $[Ca^{2+}]_i$ dynamics, reducing the frequency of local $[Ca^{2+}]_i$ release events and preventing their synchronization. This impairment inhibited the generation of Ca^{2+} transients and delayed spontaneous activity. We also used action potentials recorded in WT SAN cells as voltage-clamp commands for $Ca_v1.3^{-/-}$ cells. Although these experiments showed abolished Ca^{2+} entry through L-type Ca^{2+} channels in the diastolic depolarization range of KO SAN cells, their sarcoplasmic reticulum Ca^{2+} load remained normal. β-Adrenergic stimulation enhanced pacemaking of both genotypes, though, $Ca_v1.3^{-/-}$ SAN cells remained slower than WT. Conversely, we rescued pacemaker activity in $Ca_v1.3^{-/-}$ SAN cells and intact tissues through caffeine-mediated stimulation of Ca^{2+}-induced Ca^{2+} release.
Conclusions	$Ca_v1.3$ channels play a critical role in the regulation of $[Ca^{2+}]_i$ dynamics, providing an unanticipated mechanism for triggering local $[Ca^{2+}]_i$ releases and thereby controlling pacemaker activity. Our study also provides an additional pathophysiological mechanism for congenital SAN dysfunction and heart block linked to $Ca_v1.3$ loss of function in humans.
Keywords	Pacemaker activity • Sino-atrial node • Ca^{2+} dynamics • $Ca_v1.3$ • L-type Ca^{2+} channels

1. Introduction

Pacemaker activity of the Sino-atrial node (SAN) is a fundamental physiological function in vertebrates which is still not completely understood. Spontaneous activity is due to the diastolic depolarization phase (DDP) of the SAN action potential (AP). This phase drives the membrane voltage from the end of the repolarization to the threshold of the following AP.[1] Several ion channels participating in DDP have been characterized, and their working mechanism is generally referred to as the 'membrane clock'. These include hyperpolarization-activated 'funny' (f) HCN channels, voltage-dependent T- and L-type Ca^{2+} channels (VDCCs),[2–4] transient receptor potential (TRP) channels,[5,6] and

---

the sustained inward current (I_{st}).[7] Recent evidence also indicates that the DDP is generated through a complex interplay between 'membrane clock'[1,8] and spontaneous cyclic release of Ca^{2+} stored in the sarcoplasmic reticulum (SR).[8] According to the latter mechanism, so-called 'Ca^{2+} clock', the cyclical refilling of the SR generates spontaneous local Ca^{2+} releases (LCRs), also called Ca^{2+} sparks or wavelets, during the late DDP. Such release of Ca^{2+} in turn activates the Na^{+}/Ca^{2+} exchanger (NCX), generating a current (I_{NCX}) that allows the SAN cells to depolarize up to the threshold of the next AP.[8]

Two distinct L-type Ca^{2+} channels (LTCCs) are expressed in the SAN: $Ca_v1.2$ and $Ca_v1.3$,[3] but the latter is the predominant isoform.[3] Previous works showed that $Ca_v1.3$ channels are activated at voltages spanning the DDP range.[3] Indeed, genetic loss-of-function of $Ca_v1.3$ channels induces SAN bradycardia in mice and humans[3,9] through a mechanism that still has not been investigated directly. In a previous study in mouse SAN cells,[10] we showed that contrary to $Ca_v1.2$, $Ca_v1.3$ channels preferentially co-localize with the cardiac ryanodine receptor (RyR), suggesting their spatial proximity. Also, we demonstrated that excessive RyR-dependent Ca^{2+} release, not synchronized with the generation of Ca^{2+} transients, inactivates LTCCs in the SAN of a mouse model of human Catecholaminergic Polymorphic Ventricular Tachycardia (CPVT),[11] leading to impaired SAN pacemaker activity.

Here we show that $Ca_v1.3$ channels modulate SR Ca^{2+} release in SAN pacemaker cells, and that the impairment of such mechanism contributes to the bradycardia observed after $Ca_v1.3$ inactivation. This new regulation of RyR-dependent Ca^{2+} release underscores the importance of $Ca_v1.3$ channels for linking membrane depolarization to $[Ca^{2+}]_i$ dynamics during pacemaker activity. Also, it provides a potential pathophysiological mechanism for the sinus diseases induced by loss-of-function of this channel. Indeed, in the life-threatening autoimmune congenital heart block (CHB), anti-Ro/La (positive IgG) antibodies produced by the mother, access the fetal circulation during the gestation, causing functional inhibition of $Ca_v1.3$ channels and consequent sinus bradycardia.[12] Congenital bradycardia caused by non-functional $Ca_v1.3$ channels have been demonstrated also in the 'Sino-atrial Node Dysfunction and Deafness syndrome' (SANDD)[9] and in Ankyrin-B based SAN dysfunction.[13]

2. Methods

Detailed methods can be found in the Supplementary material online. The investigation conforms to the Guide for the Care and Use of Laboratory Animals (eighth edition, 2011), published by the US National Institute of Health and European directives (2010/63/EU) and was approved by the French Ministry of Agriculture (N° D34-172-13). Briefly, WT (C57BL6/J) and $Ca_v1.3^{-/-}$ (C57BL6/J background[3]) mice were euthanized by cervical dislocation following deep anaesthesia, consisting of 0.01 mg/g of xylazine (Rompun 2%, Bayer AG, Leverkusen Germany), 0.1 mg/g of ketamine (Imalgène, Merial, Bourgelat France), and 0.2 mg/g of Na-pentobarbital (CEVA, France). The heart was then removed and the intact SAN/atrial tissue was dissected. The SAN tissue was further digested enzymatically in order to isolate individual cells. These cells were analysed by Ca^{2+} imaging, using laser scanning confocal microscopy and Fura 2 fluorescence measurements, or by the patch-clamp technique. In the *ex vivo* experiments, we pinned the entire SAN/atrial tissue onto a Sylgard-coated glass bottom petri dish, and we analysed it by Ca^{2+} imaging. Both males and females aged 3−5 months were used with an equivalent ratio, and we did not observe any gender-specific differences. When testing statistical differences, results were considered significant with $P < 0.05$. We specify the statistical test used in each experiment in the figure legend.

3. Results

3.1 Spontaneous APs of $Ca_v1.3^{-/-}$ SAN cells

We first studied pacemaker activity in WT and $Ca_v1.3^{-/-}$ SAN cells under control conditions (Tyrode's solution) and upon β-adrenergic stimulation with isoproterenol (ISO, 10 nM; *Figure 1*). In comparison to WT, $Ca_v1.3^{-/-}$ SAN cells displayed slower spontaneous pacemaking (*Figure 1A* and *B*) and lower depolarization rates in the linear and exponential part of the DDP (*Figure 1C* and *D*). Ablation of $Ca_v1.3$ channels did not affect the AP threshold, amplitude, or upstroke velocity in SAN cells, but significantly prolonged the AP duration (see Supplementary material online, *Table S1*). Perfusion with ISO (10 nM) enhanced pacemaker activity in WT and $Ca_v1.3^{-/-}$ SAN cells, without eliminating the differences between their AP rates (*Figure 1A* and *B*). ISO (10 nM) increased the slope of the linear DDP (SLDD) in both cell groups (*Figure 1C*), but failed to increase the slope of the exponential DDP (SEDD) in $Ca_v1.3^{-/-}$ cells (*Figure 1C* and *D*, and Supplementary material online, *Figure S1A*). Thus, β-adrenergic stimulation could not rescue the effects of $Ca_v1.3$ ablation (*Figure 1D*).

We also recorded sub-threshold depolarizations of the membrane voltage that failed to trigger APs (arrow in *Figure 1A*). These events were significantly more frequent in $Ca_v1.3^{-/-}$ than in WT SAN cells (*Figure 1E*), and they were similar to the previously described Delayed After Depolarizations (DADs). DADs are provoked by abnormal $[Ca^{2+}]_i$ handling.[13,14] Thus, they could contribute to impair the automaticity of $Ca_v1.3^{-/-}$ cells. Under ISO (10 nM) DADs almost disappeared in WT, but maintained their frequency in $Ca_v1.3^{-/-}$ SAN cells (*Figure 1E*).

The high incidence of DADs in $Ca_v1.3^{-/-}$ SAN cells, together with the inefficacy of ISO (10 nM) to steepen the SEDD, were indicative of diminished efficacy of $[Ca^{2+}]_i$ handling in triggering AP in knockout (KO) cells. We thus studied $[Ca^{2+}]_i$ dynamics in WT and $Ca_v1.3^{-/-}$ SAN cells.

3.2 $Ca_v1.3$ channels stimulate local Ca^{2+} release during the diastolic phase of SAN cells

To investigate whether ablation of $Ca_v1.3$ channels altered $[Ca^{2+}]_i$ release during spontaneous activity, we studied isolated SAN cells loaded with the Ca^{2+} dye Fluo 4-AM (see Supplementary material online, *Figure S1B*), and perfused with control solution at room temperature. Under these conditions we obtained line-scan recordings (xt mode) showing Ca^{2+} release in single SAN cells. By placing the line-scan along the edge of the cells (see Supplementary material online, *Figure S1B*) we were able to record spontaneous global Ca^{2+} transients and LCRs in SAN cells of both genotypes (*Figure 2*). In few experiments, spontaneous contractions of the cells generated small invagination of Ca^{2+} signal that could be noticed on the edge of the Ca^{2+} transient in some line-scans of *Figures 2* and *6* and Supplementary material online, *Figure S5*. In WT cells we recorded LCRs similar to those previously observed in SAN cells of different mammals.[2,15,16] LCRs often occurred during the late diastolic interval preceding the Ca^{2+} transients (arrows, inset of *Figure 2A*), leading to an increase in the average fluorescence ratio (F/F_0) that we refer to as 'ramp' (*Figure 2B* and Insets).[6] Besides the LCRs generating the ramp, we recorded random LCRs loosely distributed over the full duration of the diastolic phase and apparently unrelated to the cell automaticity in both genotypes (*Figure 2A*). Ablation of $Ca_v1.3$ channels had profound consequences on $[Ca^{2+}]_i$ release.
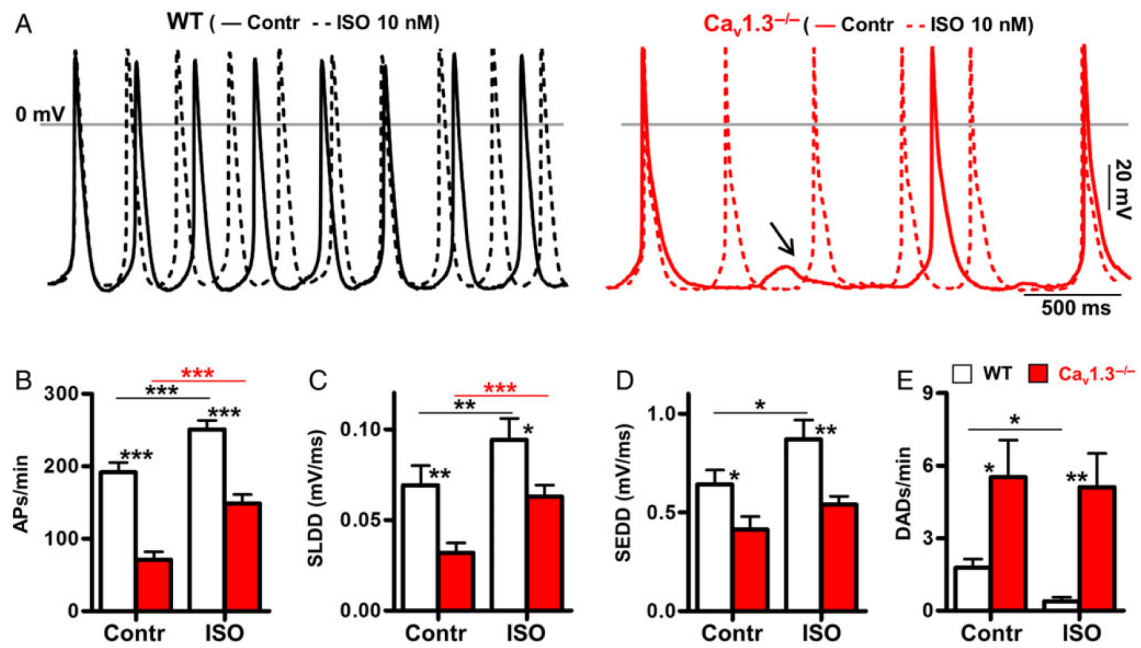
Figure 1 Spontaneous APs in single SAN cells. (*A*) APs recordings of WT and $Ca_v1.3^{-/-}$ before (Contr) and after isoproterenol (ISO 10 nM) perfusion. (*B*) APs rates and Slopes of the Linear (*C*), or Exponential (*D*) parts of the DDP (SLDD and SEDD, respectively) in WT ($n = 17$ cells from $N = 8$ mice) and $Ca_v1.3^{-/-}$ ($n = 22$ cells from $N = 7$ mice). (*E*) Frequency of DADs [arrow in (*A*)] in WT ($n = 26$ cells from $N = 15$ mice) and $Ca_v1.3^{-/-}$ ($n = 29$ cells from $N = 8$ mice). *$P < 0.05$, **$P < 0.01$, ***$P < 0.001$ by two-way ANOVA with Sidak post-test.

Under basal conditions, $Ca_v1.3^{-/-}$ cells showed reduced frequency of LCRs (ramp and loose) and spontaneous Ca^{2+} transients (*Figure 2A* and *B*). Consistent with reduced LCRs, the amplitude of the ramp in $Ca_v1.3^{-/-}$, which correlates to the amount of Ca^{2+} released during the late DDP, was lower than WT (*Figure 2C*). $Ca_v1.3^{-/-}$ SAN cells also showed higher amplitude (F/F_0) and faster slope ($\Delta F/s$) of spontaneous Ca^{2+} transients when compared with WT (*Figure 2D* and *E*, respectively). In line with these results we also observed equal amplitude and duration of LCRs in both genotypes (*Figure 2F* and *G*), but smaller LCRs width in $Ca_v1.3^{-/-}$ SAN cells (*Figure 2H*).

3.3 $Ca_v1.3^{-/-}$ SAN cells have normal SR Ca^{2+} load

The higher Ca^{2+} transient amplitude recorded in $Ca_v1.3^{-/-}$ cells could be caused by their longer cycle length (CL), so that the SR Ca^{2+}-ATPase (SERCA) pump has more time to refill the stores. To investigate SERCA activity, we estimated the SR Ca^{2+} load by rapid caffeine (Caff) application (10 mM). For this experiment, we preconditioned SAN cells of both genotypes with ISO (2 nM), in order to stimulate SERCA activity before the application of Caff (*Figure 3A*). Under these conditions WT and $Ca_v1.3^{-/-}$ cells had comparable amplitude (F/F_0) and decay (Tau) of the Caff evoked Ca^{2+} transient, suggesting equivalent SR Ca^{2+} content (*Figure 3B* and *C*). To make sure that SAN cells from both genotypes had equal possibilities to refill the SR, we performed similar experiments under control condition and simultaneous electric-field stimulation at a frequency slightly higher than the rate of spontaneous Ca^{2+} transients in WT (*Figure 3D*). In these experiments we used the ratiometric dye Fura 2 to have a quantitative measurement of Ca^{2+}. When the basal fluorescence of the stimulated Ca^{2+} transients stabilized we rapidly added 10 mM Caff (*Figure 3D*). Under this condition we recorded equivalent amplitude (F340/F380) and decay (Tau) of

the Caff-induced Ca^{2+} transients in both genotypes (*Figure 3E* and *F*, respectively). Furthermore, the fractional SR Ca^{2+} release[17] was also comparable between the two genotypes (*Figure 3G*), proving that $Ca_v1.3^{-/-}$ and WT SAN cells have equivalent SR $[Ca^{2+}]$ load, SERCA activity and NCX-mediated Ca^{2+} efflux. Therefore, we could not attribute LCRs and ramp amplitude decrease to a reduction of SR Ca^{2+} load in $Ca_v1.3^{-/-}$ cells.

3.4 $Ca_v1.3^{-/-}$ SAN cells have reduced Ca^{2+} current in the diastolic depolarization range

To investigate whether the reduction in LCRs during the DDP of $Ca_v1.3^{-/-}$ SAN cells was caused by abolition of Ca^{2+} entry via $Ca_v1.3$ channels, we performed patch-clamp whole-cell recordings of Ca^{2+} current (I_{Ca}). For this measurement, we applied as the voltage command a train of spontaneous APs previously recorded in WT cells (*Figure 4A*). We adapted extracellular and intracellular solutions to enable isolation of I_{Ca} in the absence of I_f and I_{NCX}.[3] Under these conditions, both L- and T-type Ca^{2+} currents ($I_{Ca,L}$ and $I_{Ca,T}$, respectively) could concur to generate Ca^{2+} influx via I_{Ca}. Our recordings showed I_{Ca} in WT SAN cells during the full range of voltages corresponding to the DDP and AP upstroke (*Figure 4B* and *D*). I_{Ca} density was instead significantly reduced in $Ca_v1.3^{-/-}$ cells during the same voltage ranges (*Figure 4C* and *D*). In SAN cells of both genotypes, I_{Ca} during DDP was completely blocked by application of the LTCC inhibitor nifedipine (Nife 3 μM; *Figure 4B–D*). This outcome indicated that $I_{Ca,L}$, rather than $I_{Ca,T}$, is the predominant source of Ca^{2+} entry during this AP phase. In WT cells, Ca^{2+} entry during the DDP accounted for approximately one-tenth of the total Ca^{2+} current during the full AP cycle (*Figure 4E* and *F*). This current was significantly reduced in $Ca_v1.3^{-/-}$ cells (*Figure 4E*), demonstrating that loss of $Ca_v1.3$-mediated $I_{Ca,L}$ reduced Ca^{2+} influx during the diastole of SAN cells. Although reduced,
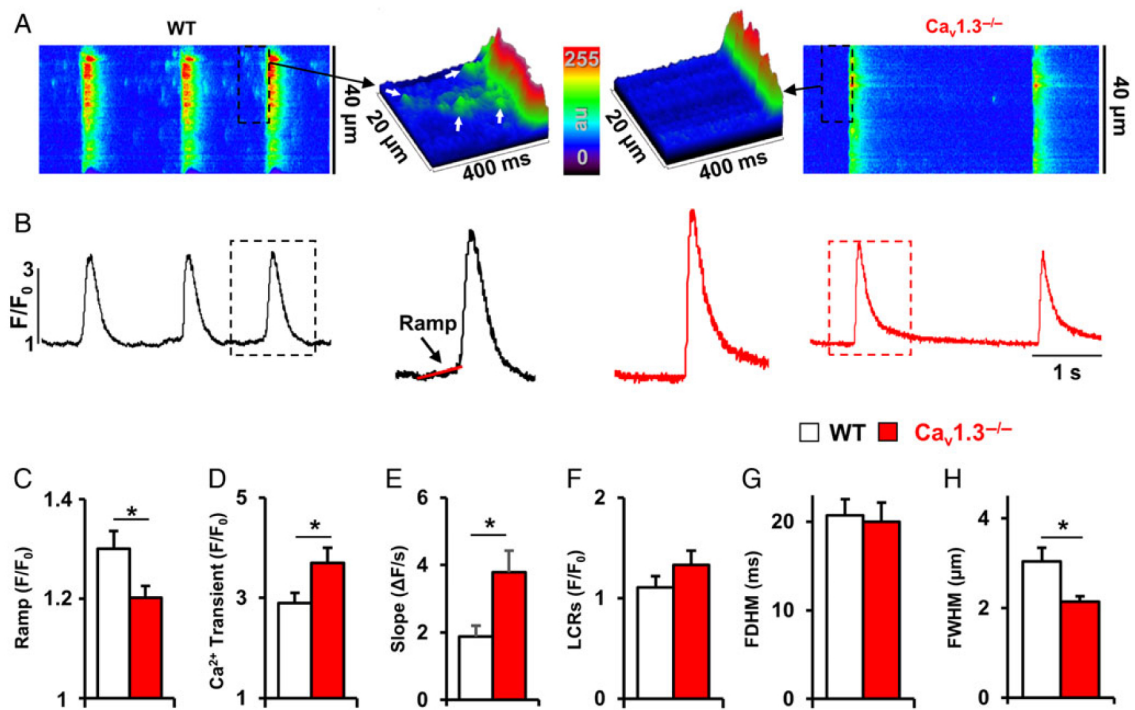
Figure 2 $[Ca^{2+}]_i$ release in single SAN cells. (A) Line-scan of WT and $Ca_v1.3^{-/-}$ single SAN cells. Insets: 3D reconstruction of diastolic $[Ca^{2+}]_i$ release. a.u. = arbitrary units. White arrows indicate late diastolic LCRs. (B) Time-course of Ca^{2+} fluorescence recorded in (A). Insets: magnified Ca^{2+} transient of both genotypes. Note the ramp in WT (red line). (C) Amplitude of the ramp in WT ($n = 10$ cells from $N = 7$ mice) and $Ca_v1.3^{-/-}$ ($n = 13$ cells from $N = 9$ mice). (D) Amplitude of the Ca^{2+} transients in WT ($n = 32$ cells from $N = 16$ mice) and $Ca_v1.3^{-/-}$ ($n = 33$ cells from $N = 16$ mice). (E) Slope of Ca^{2+} transient upstroke ($\Delta F/s$) in WT ($n = 11$ cells from $N = 6$ mice) and $Ca_v1.3^{-/-}$ ($n = 18$ cells from $N = 6$ mice). (F–H) amplitude, full duration, and full width at half maximum (F/F_0, FDHM and FWHM, respectively) of LCRs recorded in WT ($n = 10$ cells from $N = 6$ mice) and $Ca_v1.3^{-/-}$ ($n = 19$ cells from $N = 6$ mice). *$P < 0.05$ by unpaired t-test.

in $Ca_v1.3^{-/-}$ cells the Ca^{2+} influx during the upstroke was still maintained by $Ca_v1.2$ allowing APs generation and SR refilling.

3.5 $Ca_v1.3$ channels are required to synchronize LCRs under β-adrenergic activation

We then studied how ablation of $Ca_v1.3$ channels affected the β-adrenergic regulation of $[Ca^{2+}]_i$ release. In WT SAN cells, saturating concentration of ISO (10 nM) increased the rate of spontaneous Ca^{2+} transients and the frequency of LCRs during the entire diastolic interval (*Figure 5A–D*). $Ca_v1.3^{-/-}$ SAN cells also responded to the β-adrenergic stimulation, but without reaching the frequency of LCRs and Ca^{2+} transients recorded in WT (*Figure 5A–D*). To investigate whether the β-adrenergic pathway affected specifically the LCRs occurring in the late diastolic phase, we analysed the ramp of spontaneous Ca^{2+} transients stimulated with ISO (10 nM). In WT, this treatment appeared to organize the LCRs in a more compact ramp (*Figure 5A*) that presumably stimulated the pacemaker depolarization.[8] This effect was not observed in $Ca_v1.3^{-/-}$ SAN cells, where we recorded increased number of LCRs under ISO (10 nM), but spread along the entire diastolic interval (*Figure 5B*). To further investigate this issue, we correlated the ramp length with its amplitude (F/F_0) before and after ISO (10 nM) stimulation (*Figure 5E and F*). We found a significant increase in the slope of the linear regression only after ISO (10 nM) stimulation in WT, but not in $Ca_v1.3^{-/-}$. Therefore, we

conclude that ablation of $Ca_v1.3$ channels prevented normal synchronization of LCRs under β-adrenergic stimulation, delaying triggering of spontaneous Ca^{2+} transients.

3.6 $Ca_v1.3$ ablation promotes irregular spontaneous activity and formation of $[Ca^{2+}]_i$ waves in the intact SAN tissue

In $Ca_v1.3^{-/-}$ SAN cells we observed several DADs-like events that could not be suppressed by ISO (*Figure 1*). As shown in previous studies, $[Ca^{2+}]_i$ waves and DADs impaired pacemaker activity, preventing impulse formation in the intact SAN tissue, and inducing bradycardia.[14,18] We thus hypothesized that the absence of $Ca_v1.3$-mediated Ca^{2+} influx prevents normal depolarization of SAN cells through NCX, promoting formation of DADs and $[Ca^{2+}]_i$ waves, and contributing to bradycardia in $Ca_v1.3^{-/-}$ SAN tissue. To test this hypothesis, we studied $[Ca^{2+}]_i$ release in individual cells within the central pacemaker region of the intact SAN tissue[11] (*Figure 6A and B*; Supplementary material online, *Figure S2A and B*).

The rate of spontaneous Ca^{2+} transients in WT tissues was comparable with our previous studies.[11] Instead, pacemaker activity of $Ca_v1.3^{-/-}$ SAN tissue was significantly slower (*Figure 6C*). Individual cells within the central region of $Ca_v1.3^{-/-}$ SANs were also characterized by higher incidence of $[Ca^{2+}]_i$ waves (*Figure 6B and D*). This abnormal $[Ca^{2+}]_i$ release translated into slow and irregular spontaneous pacing in $Ca_v1.3^{-/-}$ SAN tissues, as shown by the higher coefficient
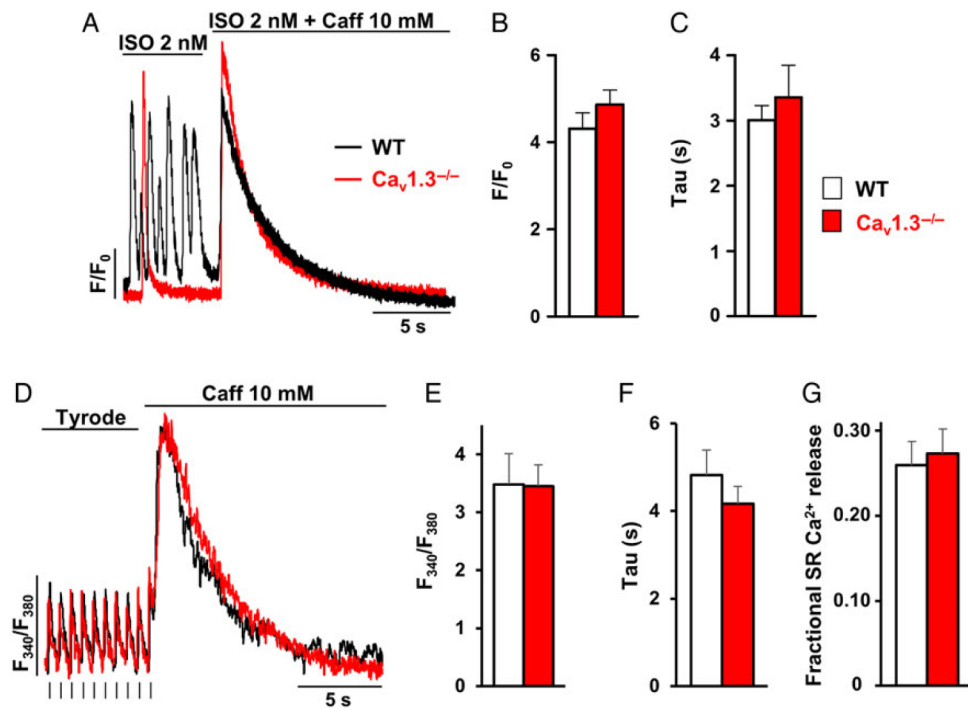
Figure 3 SR Ca^{2+} load in single SAN cells. (*A*) Time-courses of Ca^{2+} fluorescence generated by Fluo 4 in WT and $Ca_v1.3^{-/-}$ single SAN cells exposed to ISO (2 nM) and then to saturating concentration of caffeine (Caff, 10 mM). (*B* and *C*) amplitudes and recovery time of the Caff-induced Ca^{2+} transient in WT ($n = 17$ cells from $N = 8$ mice) and $Ca_v1.3^{-/-}$ ($n = 17$ cells from $N = 7$ mice). (*D*) Time-courses of Ca^{2+} fluorescence quantified by Fura 2 in WT and $Ca_v1.3^{-/-}$ single SAN cells, before and after exposure to high concentration of Caff (10 mM). Black ticks indicate electric-field stimulation at 1.5 Hz. (*E–G*) Amplitudes, recovery time, and fractional SR Ca^{2+} release of the Caff-induced Ca^{2+} transient in WT ($n = 11$ cells from $N = 3$ mice) and $Ca_v1.3^{-/-}$ ($n = 15$ cells from $N = 3$ mice).

of variation (CF) of the Ca^{2+} transients CL (*Figure 6F*). Perfusion with ISO (20 nM) increased the frequency of spontaneous Ca^{2+} transients in both genotypes (*Figure 6C*). However, it did not eliminate the difference between $Ca_v1.3^{-/-}$ and WT, nor it regularised spontaneous pacing in KO tissues (*Figure 6B* and *F*). Possibly as a consequence of the faster and more organized activity, in the SAN cells analysed within the SAN tissue of both genotypes, we recorded ~10 times less LCRs than in isolated SAN cells. In this experiment, we neither observed significant increase of LCRs after ISO stimulation, as previously reported[11] (*Figure 6E*).

3.7 Direct conditioning of RyR-dependent $[Ca^{2+}]_i$ release restored pacemaker activity of $Ca_v1.3^{-/-}$

We observed a clear decrease of LCRs frequency in $Ca_v1.3^{-/-}$ SAN cells (*Figures 2* and *5*). Therefore, we hypothesized that in WT SAN cells, $Ca_v1.3$ channels stimulate RyRs through a mechanism of Ca^{2+}-induced Ca^{2+} release (CICR) during the late DDP. This is a likely mechanism, possibly allowed by the physical proximity between $Ca_v1.3$ channels and RyRs.[10] A similar mechanism, but regulated by $Ca_v1.2$ channels, has also been demonstrated in contractile myocytes.[19,20] Furthermore, using a protocol of ramp depolarization to mimic DDP of single SAN cells, it has been demonstrated generation and synchronization of LCRs in whole Ca^{2+} transients at voltages consistent with $Ca_v1.3$ activation.[15] We thus tested our hypothesis by inducing CICR via direct conditioning of RyRs in the absence of $Ca_v1.3$.[21] For this purpose, we

facilitated RyR opening in single SAN cells by non-saturating [Caff] (200 μM) application (*Figure 7*). SAN cells were first exposed to saturating [ISO] (10 nM), to maximally activate the cAMP- and PKA-dependent stimulation of $[Ca^{2+}]_i$ release and Ca^{2+} reuptake in the SR.[22] As indicated above, this treatment did not rescue the impaired pacemaker activity of $Ca_v1.3^{-/-}$ SAN cells (*Figure 5*). We then perfused low [Caff] (200 μM) that did not elicit SR Ca^{2+} depletion in WT SAN cells. This RyRs conditioning did not change the rate of spontaneous Ca^{2+} transients in WT (*Figure 7A* and *B*), and caused only a fast alteration of their diastolic $[Ca^{2+}]_i$ ($[Ca^{2+}]_{Diastol}$) that quickly recovered to control levels (dashed line in *Figure 7A* and *C*), similarly to what has been shown in ventricular myocytes.[23] In contrast, $Ca_v1.3^{-/-}$ SAN cells robustly responded to Caff (200 μM) by raising their $[Ca^{2+}]_{Diastol}$ and increasing the spontaneous Ca^{2+} transient frequency to levels similar to WT (*Figure 7A–C*). The Caff-mediated recovery in single $Ca_v1.3^{-/-}$ SAN cells was maintained as long as the $[Ca^{2+}]_{Diastol}$ remained elevated.

We then investigated whether conditioning of RyRs could rescue the generation of spontaneous Ca^{2+} transients also in the intact $Ca_v1.3^{-/-}$ SAN tissues. We thus stimulated both genotypes with ISO (20 nM). Then, similarly to our approach in isolated cells, we conditioned the SAN tissues with a low dose of Caff that did not completely deplete the SR in WT (*Figure 7D*). Possibly because of the complex structural organization of the intact SAN, we found that the [Caff] needed in tissue (1 mM) was higher than that employed in isolated cells (200 μM). Similarly to what observed in isolated $Ca_v1.3^{-/-}$ SAN cells, individual cells inside the intact KO SAN tissue displayed strong responsiveness to Caff (1 mM), reaching the same frequency of spontaneous Ca^{2+}
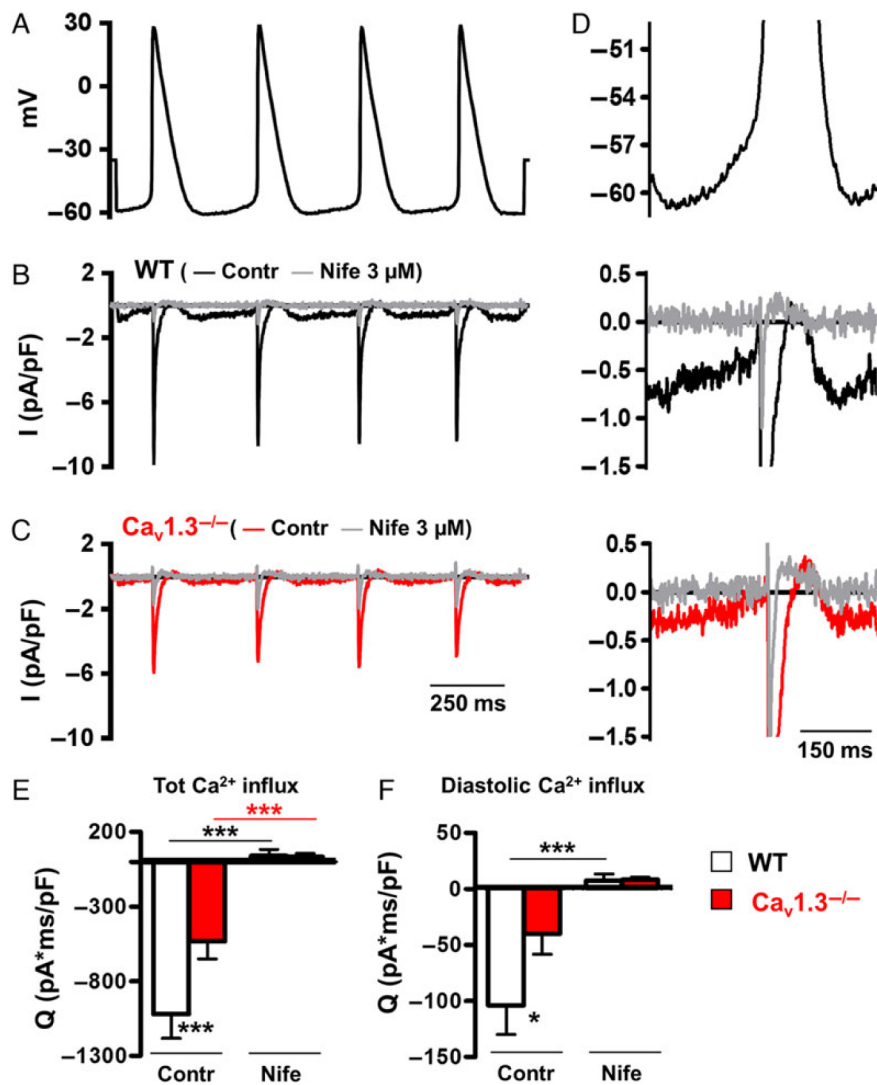
Figure 4 $Ca_v1.3$-mediated $I_{Ca,L}$ activated during the AP cycle. (A) AP sample applied as voltage command. (B and C) Sample traces of the corresponding net I_{Ca} in WT and $Ca_v1.3^{-/-}$ before (Contr) and after nifedipine (Nife, 3 μM) perfusion. (D) Magnification of the second AP in (A) with the respective currents recorded in (B) and (C). (E) Total Ca^{2+} influx via I_{Ca} recorded during the whole AP cycle in WT ($n = 8$ cells from $N = 3$ mice) and $Ca_v1.3^{-/-}$ ($n = 8$ cells from $N = 2$ mice). (F) Diastolic Ca^{2+} influx via I_{Ca} recorded as in (E). *$P < 0.05$, ***$P < 0.001$ by two-way ANOVA with Sidak post-test.

transients recorded in WT (*Figure 7D and E*). Also in these experiments, $Ca_v1.3^{-/-}$ SAN tissues generally showed rise of the $[Ca^{2+}]_{Diastol}$ and reduction of the systolic peak under Caff (1 mM) comparable with single $Ca_v1.3^{-/-}$ SAN cells (see Supplementary material online, *Figure S3*). Despite the strong increase of LCRs frequency, Caff-treated WT cells within the intact SAN tissue did not augment, the frequency of spontaneous Ca^{2+} transients (*Figure 7D and E*). Instead, Caff-treated $Ca_v1.3^{-/-}$ SANs generated copious $[Ca^{2+}]_i$ waves (*Figure 7D* and Supplementary material online, *Figure S3*). In these tissues, comparing 5 and 25 s after Caff (1 mM) exposure (see Supplementary material online, *Figure S3*), we found $\sim$25% increase of $[Ca^{2+}]_i$ waves frequency ($n = 5$ mice; *$P < 0.01$ by paired t-test). These waves tended also to decrease their amplitude and to come close or merge with the Ca^{2+} transients. Indeed, we found $\sim$70% reduction in the time-lapse between $[Ca^{2+}]_i$ waves and the following Ca^{2+} transient after Caff (1 mM) perfusion (see Supplementary material online, *Figures S3 and S4*). This observation suggested that conditioning of RyR-dependent Ca^{2+} release by Caff was

synchronizing $[Ca^{2+}]_i$ waves with Ca^{2+} transients to restore the frequency of spontaneous automaticity with a dynamic similar to that observed in isolated SAN cells.

3.8 Phosphodiesterase inhibition did not recover $Ca_v1.3^{-/-}$ SAN cells pacemaker activity

Since Caff is a methylxanthine, besides conditioning the RyR-dependent $[Ca^{2+}]_i$ release, it could directly inhibit phosphodiesterase (PDE) activity, determining an increase of the intracellular [cAMP] higher than after ISO (10 nM) perfusion. IBMX is a potent inhibitor of all PDE isoforms, reported to enhance the automaticity of SAN cells.[24,25] Therefore, we used this drug to test whether rescuing of the Ca^{2+} transient frequency in $Ca_v1.3^{-/-}$ cells was caused by inhibition of PDEs activity. In spite of IBMX (100 μM) addition, ISO-treated cells isolated from either WT or $Ca_v1.3^{-/-}$ SAN did not further change the
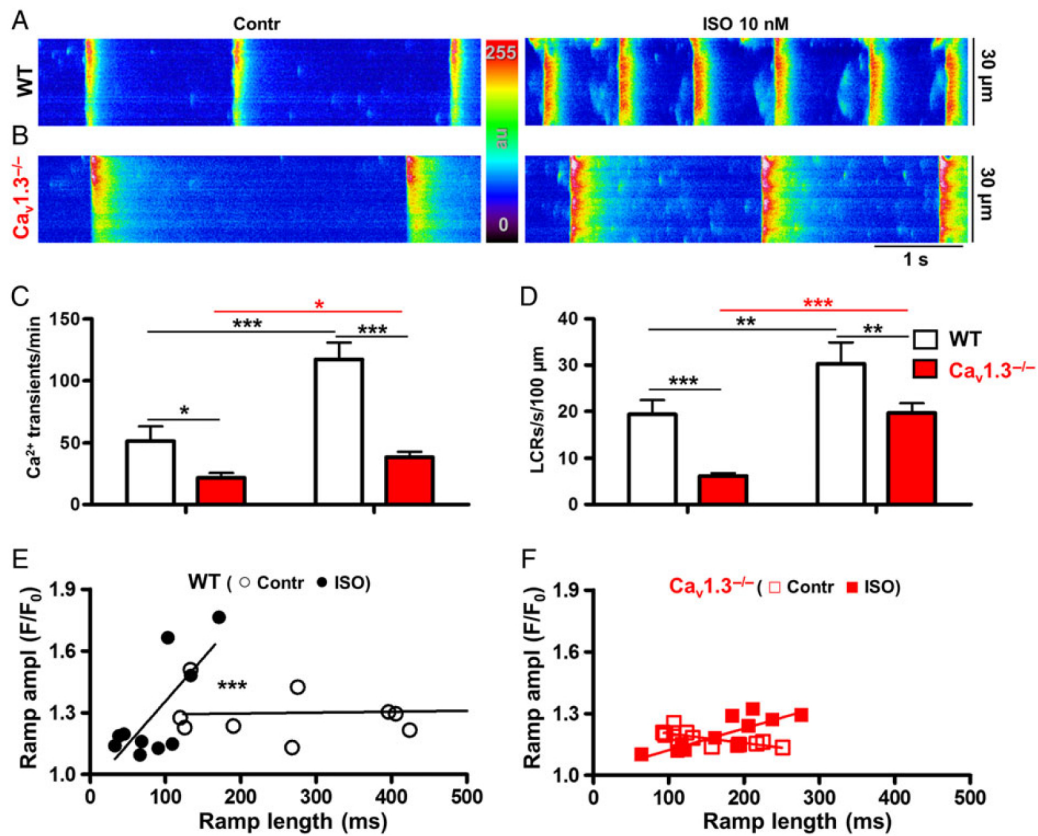
Figure 5 Synchronization of LCRs under β-adrenergic stimulation. (*A* and *B*) Line-scan of single SAN cells before (Contr) and after ISO (10 nM) stimulation. (*C*) Frequency of spontaneous Ca^{2+} transients in WT ($n = 11$ cells from $N = 6$ mice) and $Ca_v1.3^{-/-}$ ($n = 21$ cells from $N = 6$ mice). (*D*) Frequency of LCRs, normalized to 100 μm of line-scan length, in WT ($n = 8$ cells from $N = 6$ mice) and $Ca_v1.3^{-/-}$ ($n = 19$ cells from $N = 5$ mice). (*E* and *F*) Correlation between ramp amplitude (ratio between the fluorescence at the end and at the beginning of the ramp) and ramp length (interval between the beginning and the end of the ramp) in WT ($n = 10$ cells from $N = 7$ mice) and $Ca_v1.3^{-/-}$ ($n = 12$ cells from $N = 4$ mice). (*C* and *D*) *$P < 0.05$, **$P < 0.01$, ***$P < 0.001$ by two-way ANOVA with Bonferroni's post-test. (*E*) ***$P < 0.001$ by one-way ANOVA with Tukey's post-test of the angular coefficients of the linear regressions.

frequency of spontaneous Ca^{2+} transients (see Supplementary material online, *Figure S5*). Instead, only $Ca_v1.3^{-/-}$ SAN cells showed a significant increment in the frequency of Ca^{2+} transients under concomitant perfusion of IBMX (100 μM) and Caff (200 μM; Supplementary material online, *Figure S5*).

4. Discussion

We have previously shown that $Ca_v1.3$-mediated $I_{Ca,L}$ is activated at voltages spanning the DDP of SAN cells and play a key role during their spontaneous depolarization.[3] In line with these earlier observations, here we found that $Ca_v1.3$ channels generate most of the $I_{Ca,L}$-mediated inward current during the DDP (*Figure 4*). Furthermore, we reported that ablation of $Ca_v1.3$ channels reduces the DDP slope, both in the linear and in the exponential segment.

In this study, we highlighted a new and unexpected role for $Ca_v1.3$ channel in pacemaker activity. Indeed, our results suggest that the local increase of $[Ca^{2+}]_i$ generated by $Ca_v1.3$ Ca^{2+} current induces RyR opening, thereby favouring the coupling between membrane depolarization and SR Ca^{2+} release. Thus, $Ca_v1.3$ channels appear to be the main trigger of LCRs generation in the late DDP. Through

this mechanism, $Ca_v1.3$ could stimulate the NCX-mediated depolarizing current, helping to reach the voltage threshold necessary to trigger an AP. In this respect, we showed that $Ca_v1.3$ ablation reduces LCRs occurrence, particularly at the end of the DDP, reducing the amplitude of the $[Ca^{2+}]_i$ ramp and impairing the generation of Ca^{2+} transients. This impairment could determine the generation of the DADs reported in this manuscript, and in a mouse model of Ankyrin-B deficiency showing disrupted $Ca_v1.3$ trafficking to the membrane.[13,26]

$Ca_v1.3$ channels co-localize with RyRs,[10] and together with NCX they have been located in the caveolae, where they are probably anchored by Ankyrin-B proteins.[26,27] Therefore, these channels could induce the increase in $[Ca^{2+}]_{Diastol}$ necessary to stimulate CICR and the consequent activation of NCX. Consistent with this mechanism we were able to recover $Ca_v1.3^{-/-}$ automaticity only by direct stimulation of RyR-dependent $[Ca^{2+}]_i$ release. We also found that maximal β-adrenergic activation and PDEs inhibition could not rescue the spontaneous pacemaker activity of $Ca_v1.3^{-/-}$ SAN. This observation indicates that stimulation of other mechanisms involved in pacemaker activity such as I_f or the crosstalk between spontaneous diastolic LCRs and I_{NCX}[16] cannot compensate for the absence of $Ca_v1.3$ channels.
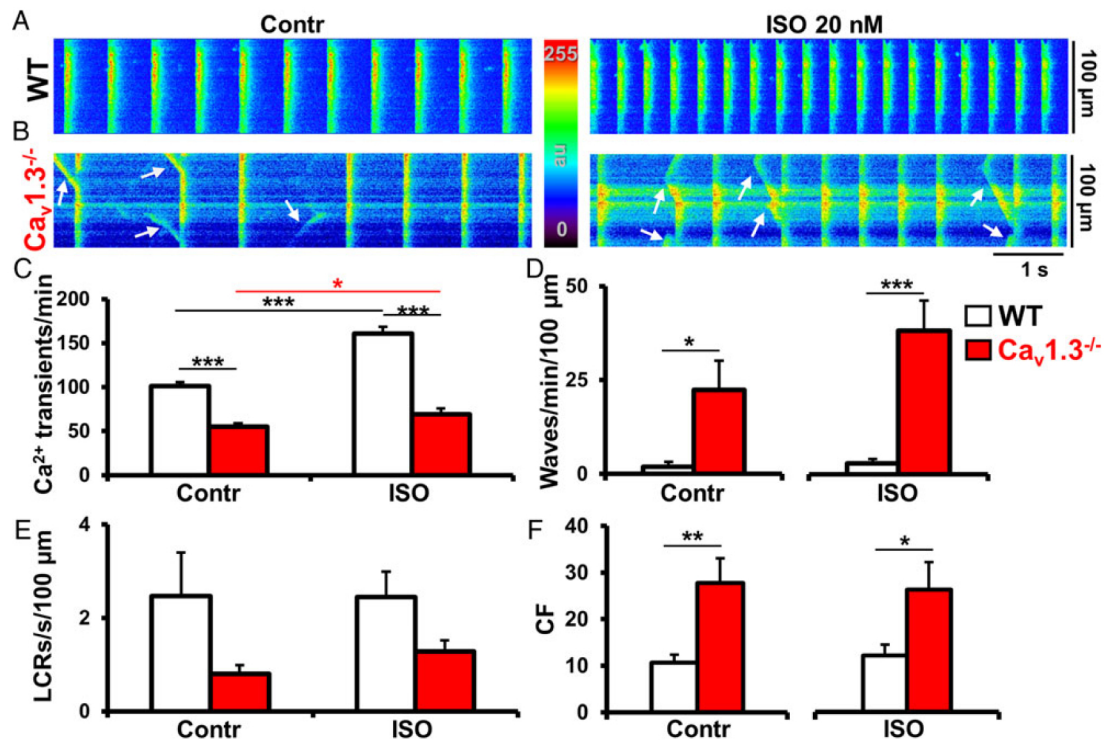
Figure 6 $[Ca^{2+}]_i$ release in individual cells of the central pacemaker region of the intact SAN. (*A* and *B*) Line-scans of WT and $Ca_v1.3^{-/-}$ SAN cells within the intact SAN before (Contr) and after ISO (20 nM) perfusion. Arrows indicate $[Ca^{2+}]_i$ waves. Frequency of Ca^{2+} transients (*C*), $[Ca^{2+}]_i$ waves (*D*), and LCRs (*E*) in WT (N = 5 SAN tissues; at least three cells per tissue), and $Ca_v1.3^{-/-}$ (N = 9 SAN tissues; at least three cells per tissue). (*F*) Coefficient of variation of Ca^{2+} transient generation (CF = StD/mean of CL) in WT (n = 23 cells in Contr and 15 in ISO from N = 5 SAN tissues) and $Ca_v1.3^{-/-}$ (N = 27 cells in Contr and 18 in ISO from N = 5 SAN tissues). *P < 0.05, **P < 0.01, ***P < 0.001 by unpaired *t*-test and two-way ANOVA with Holm−Sidak's post-test.

4.1 $Ca_v1.3$ channels are important inducers of diastolic LCRs

In primary SAN pacemaker cells diastolic LCRs have been predominantly attributed to spontaneous, cyclical, and voltage-independent SR Ca^{2+} release by RyRs.[8] However, two studies in SAN cells reported a dependency of LCRs on membrane potential, at voltages as negative as −50 mV.[2,15] This voltage is compatible with activation of both $Ca_v3.1$-mediated $I_{Ca,T}$ and $Ca_v1.3$-mediated $I_{Ca,L}$ in SAN cells. Consistently with the hypothesis that $Ca_v1.3$ induces LCRs generation, in $Ca_v1.3^{-/-}$ SAN cells LCRs frequency was reduced. This reduction was particularly evident during the late DDP, as indicated by the lower $[Ca^{2+}]_i$ ramp amplitude.

$I_{Ca,T}$ density is not affected by $Ca_v1.3$ inactivation.[3] Therefore, we do not exclude the presence of $Ca_v3.1$-,[2] spontaneous,[8] or $Ca_v1.2$-induced LCRs in SAN cells of both genotypes. These mechanisms could account for the residual LCRs observed in $Ca_v1.3^{-/-}$ SAN cells, especially under ISO perfusion. Indeed, under β-adrenergic stimulation the RyRs are more sensitive to Ca^{2+}[28] and the activation threshold of $Ca_v1.2$ channels is shifted negatively by 5 mV.[3] Nevertheless, the involvement of $Ca_v3.1$ channels in LCRs induction has been challenged in rabbit SAN cells, in which exposure to 50 μM Ni^{2+} did not affect the number of LCRs.[29] In both genotypes, we possibly recorded spontaneous LCRs, during the time-lapse preceding the ramp. These spontaneous LCRs could be generated by a stochastic opening of RyRs and did not show obvious relationship with the phase of pacemaker activity.

Instead, the comparison between the $[Ca^{2+}]_i$ ramp amplitude in WT and $Ca_v1.3^{-/-}$ SAN cells clearly indicated that the LCRs generation during the late DDP were specifically reduced by the ablation of $Ca_v1.3$ channels. The smaller LCR's width recorded in KO SAN cells could be also explained by requirement of $Ca_v1.3$ in the excitation of larger RyR clusters during CICR. It is unlikely that loss of LCRs in $Ca_v1.3^{-/-}$ SAN cells was due to a general remodelling of the Ca^{2+} release machinery. Indeed, KO SAN cells presented normal SR Ca^{2+} content and reuptake, indicating a direct link between absence of $Ca_v1.3$ and the reduction of LCRs.

4.2 β-Adrenergic stimulation synchronizes LCRs during the late DDP

Previous reports on contractile cardiomyocytes showed that the β-adrenergic stimulation increases the synchronization of LCRs in response to LTCCs opening.[30−32] In mouse SAN cells, it has also been shown that a voltage protocol eliciting maximal LTCCs activation, synchronizes most LCRs into a cell-wide Ca^{2+} transient.[15] Since β-adrenergic stimulation shifts the threshold of LTCCs opening by −5 mV, determining an earlier $I_{Ca,L}$ activation,[3] we can expect that perfusion with ISO enhances synchronization of LCRs in WT. We observed an increase in LCRs frequency and spontaneous Ca^{2+} transients in both WT and KO SAN cells under ISO (10 nM) stimulation. Nevertheless, the rate of spontaneous Ca^{2+} transients in $Ca_v1.3^{-/-}$ SAN cells never reached the level of WT. Indeed, ablation
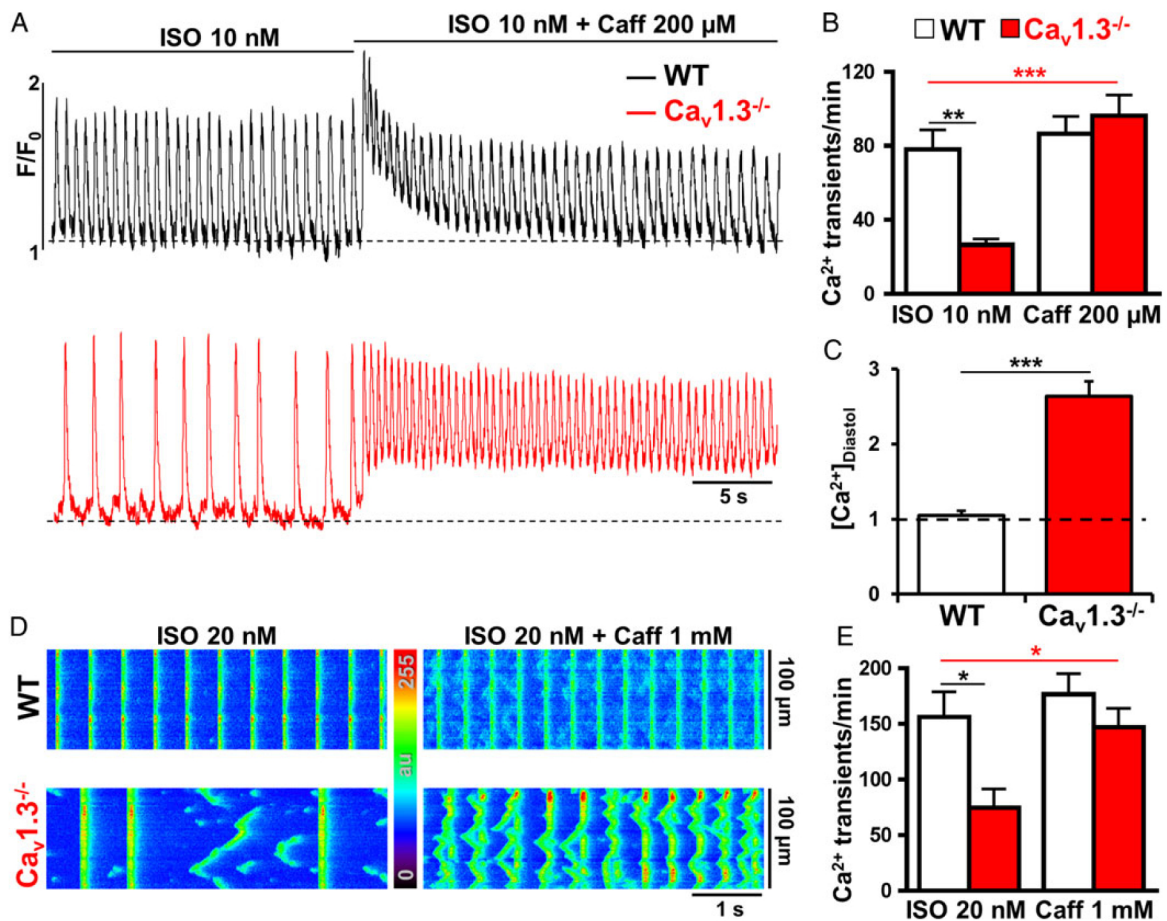
Figure 7 Direct conditioning of Ca^{2+} induced Ca^{2+} release. (A) Examples of time-course Ca^{2+} fluorescence in isolated WT and $Ca_v1.3^{-/-}$ single SAN cells preconditioned with ISO (10 nM), before and after perfusion with low [Caff] (200 μM). Dashed lines highlight $[Ca^{2+}]_{Diastol}$ before Caff (200 μM) perfusion. (B) Frequency of spontaneous Ca^{2+} transients in single WT ($n = 6$ cells from $N = 4$ mice) and $Ca_v1.3^{-/-}$ ($n = 7$ cells from $N = 3$ mice) SAN cells treated as in (A). (C) Changes in basal diastolic $[Ca^{2+}]i$ ($[Ca^{2+}]Diastol$) in WT ($n = 6$ cells from $N = 4$ mice) and Cav1.3$^{-/-}$ ($n = 7$ cells from $N = 3$ mice) after perfusion with Caff (200 μM). Values on the y-axis were normalized to the $[Ca^{2+}]_{Diastol}$ (dashed line) measured before Caff (200 μM) perfusion. (D) Line-scan recorded in the SAN tissue pacemaker region before and after perfusion with Caff (1 mM). (E) Frequency of spontaneous Ca^{2+} transients in SAN tissue of WT ($n = 6$) and $Ca_v1.3^{-/-}$ ($N = 8$) treated as in (D). *$P < 0.05$, **$P < 0.01$, ***$P < 0.001$ by two-way ANOVA with Bonferroni's post-test and unpaired t-test.

of $Ca_v1.3$ channels impaired the synchronization of LCRs under ISO (10 nM) stimulation (*Figure 5F*). Thus, this treatment increased the total number of LCRs recorded in $Ca_v1.3^{-/-}$ SAN cells, but failed to synchronize the LCRs constituting the ramp. These findings indicate that the ISO-mediated synchronization of LCRs strongly increased the likelihood of triggering a whole-cell Ca^{2+} transient in SAN cells, and highlight the requirement of $Ca_v1.3$ channels for such synchronization. Consistent with these findings, ISO did not increase the slope of the exponential DDP in $Ca_v1.3^{-/-}$ SAN cells.

4.3 Caffeine-mediated increase of $[Ca^{2+}]_{Diastol}$ rescued the effects of $Ca_v1.3$ ablation on $[Ca^{2+}]_i$ release

Our results indicating $Ca_v1.3$ channels as the inducer of LCRs during the DDP, are consistent with the normal activation range of $Ca_v1.3$. Also they agree with the rescuing of pacemaker activity obtained during direct stimulation of CICR in $Ca_v1.3^{-/-}$ SAN cells. Further studies will be

necessary to investigate the exact mechanism by which CICR rescued pacemaker activity of $Ca_v1.3^{-/-}$ SAN cells. However, we hypothesize that the Caff-induced opening of RyRs promotes increase of $[Ca^{2+}]_{Diastol}$ (*Figure 7A* and *E*), mimicking the normal $Ca_v1.3$-mediated induction of RyR Ca^{2+} release. This $[Ca^{2+}]_{Diastol}$ increase may activate INCX, as shown in ventricular myocytes.[23] Also, it might stimulate the Ca^{2+} activated Adenylate Cyclase 1 and 8,[33] increasing the phosphorylation state of $Ca_v1.3^{-/-}$ SAN cells. These modulations could promote SAN cell diastolic depolarization, helping to quickly reach the AP threshold, and accelerating SAN automaticity. In this respect, it has been recently reported that L-type agonist BayK8644 increases I_{NCX} in mouse SAN cells, indicating a direct link between LTCCs opening and NCX activation.[34] Also, increase in the global $[Ca^{2+}]_{Diastol}$ and consequent enhancement of pacemaker activity has been reported in cardiomyocytes derived from human induced pluripotent stem cells perfused with low dose of Caff, comparable with ours.[35] NCX-mediated Ca^{2+} extrusion during continuous Caff (200 μM) exposure could cause partial SR depletion[23] and consequent decrease of the systolic Ca^{2+} transients amplitude

(*Figure 7A* and Supplementary material online, *Figure S3*). However, $[Ca^{2+}]_{Diastol}$ could be maintained high by the increased frequency of Ca^{2+} transients (*Figure 7A* and *E*) and the simultaneous SR Ca^{2+} refill activity SERCA-mediated.

Our Caff-mediated rescue of pacemaking in $Ca_v1.3^{-/-}$ SAN cells demonstrated that RyRs are functional in KO SAN cells. Nevertheless, the absence of $Ca_v1.3$ channels reduces RyRs open probability, slowing and disorganizing SAN automaticity in KO cells. As shown above, this impairment could not be restored by β-adrenergic stimulation nor PDEs inhibition. Interestingly, the onset of Caff effect was immediate and faster than that of ISO, supporting direct activation of RyRs. Surprisingly, the increase of LCRs recorded in individual cells of intact WT SAN tissue did not affect the frequency of spontaneous Ca^{2+} transients. This result may appear paradoxical according to the 'Ca^{2+} clock' models of pacemaking, but it could be determined by saturation of NCX activity under maximal β-adrenergic activation.

5. Conclusions

Our study shows, for the first time, a critical role for $Ca_v1.3$-mediated $I_{Ca,L}$ in regulating $[Ca^{2+}]_i$ release of SAN pacemaker cells. We demonstrated that $Ca_v1.3$ channels stimulate and synchronize RyR-dependent $[Ca^{2+}]_i$ release during normal SAN pacemaker activity. Given the dual role of $Ca_v1.3$-mediated $I_{Ca,L}$ in driving inward current in the DDP and stimulate RyR-dependent $[Ca^{2+}]_i$ release, it is tempting to speculate that these channels constitute an unexplored functional bridge between 'Ca^{2+} clock' and 'Membrane clock'.

Our work also brings new insights into the mechanisms of congenital SAN dysfunction. Indeed, lack of functional $Ca_v1.3$ channels have been implicated in the sinus bradycardia observed in the life-threatening autoimmune CHB, in the 'Sino-atrial Node Dysfunction and Deafness syndrome' (SANDD),[9] and in Ankyrin-B based SAN dysfunction.[13]

6. Limitations

The regulation of the AP waveform of mouse SAN cells requires the contribution of I_{Ca}, and the fast Na$^+$ current (I_{Na}).[1] Although this could be a limitation, we did not measure I_{Na} in $Ca_v1.3^{-/-}$ SAN cells, because KO cells displayed AP upstrokes similar to those of WT. More generally, it is possible that compensatory mechanisms secondary to $Ca_v1.3$ inactivation are involved in the pacemaker activity of $Ca_v1.3^{-/-}$ mice. In addition, we cannot exclude that the slight increase in AP duration recorded in $Ca_v1.3^{-/-}$ SAN cells might affect the following DDP phase. To avoid artefacts in $[Ca^{2+}]_i$ measurement caused by the small invagination of Ca^{2+} signal visible on the edge of some Ca^{2+} transient, we generated Ca^{2+} fluorescence time-course traces by selecting the entire line-scan except the small portion interested by these small invaginations. To evaluate the Ca^{2+} stored in the SR, we chose to directly record the peak Fura 2 florescence of the caffeine-induced Ca^{2+} transient, rather than measuring I_{NCX} in voltage clamped SAN cells.

References
1. Mangoni ME, Nargeot J. Genesis and regulation of the heart automaticity. *Physiol Rev* 2008;**88**:919–982.
2. Huser J, Blatter LA, Lipsius SL. Intracellular Ca^{2+} release contributes to automaticity in cat atrial pacemaker cells. *J Physiol* 2000;**524**:415–422.
3. Mangoni ME, Couette B, Bourinet E, Platzer J, Reimer D, Striessnig J, Nargeot J. Functional role of L-type Cav1.3 Ca^{2+} channels in cardiac pacemaker activity. *Proc Natl Acad Sci USA* 2003;**100**:5543–5548.
4. Mangoni ME, Traboulsie A, Leoni AL, Couette B, Marger L, Le Quang K, Kupfer E, Cohen-Solal A, Vilar J, Shin HS, Escande D, Charpentier F, Nargeot J, Lory P. Bradycardia and slowing of the atrioventricular conduction in mice lacking CaV3.1/alpha1G T-type calcium channels. *Circ Res* 2006;**98**:1422–1430.
5. Demion M, Bois P, Launay P, Guinamard R. TRPM4, a Ca^{2+}-activated nonselective cation channel in mouse sino-atrial node cells. *Cardiovasc Res* 2007;**73**:531–538.
6. Sah R, Mesirca P, Van den Boogert M, Rosen J, Mably J, Mangoni ME, Clapham DE. Ion channel-kinase TRPM7 is required for maintaining cardiac automaticity. *Proc Natl Acad Sci USA* 2013;**110**:E3037–E3046.
7. Cho H-S, Takano M, Noma A. The electrophysiological properties of spontaneously beating pacemaker cells isolated from mouse sinoatrial node. *J Physiol* 2003;**550**:169–180.
8. Lakatta EG, Maltsev VA, Vinogradova TM. A coupled SYSTEM of intracellular Ca^{2+} clocks and surface membrane voltage clocks controls the timekeeping mechanism of the heart's pacemaker. *Circ Res* 2010;**106**:659–673.
9. Baig SM, Koschak A, Lieb A, Gebhart M, Dafinger C, Nurnberg G, Ali A, Ahmad I, Sinnegger-Brauns MJ, Brandt N, Engel J, Mangoni ME, Farooq M, Khan HU, Nurnberg P, Striessnig J, Bolz HJ. Loss of Ca(v)1.3 (CACNA1D) function in a human channelopathy with bradycardia and congenital deafness. *Nat Neurosci* 2011;**14**:77–84.
10. Christel CJ, Cardona N, Mesirca P, Herrmann S, Hofmann F, Striessnig J, Ludwig A, Mangoni ME, Lee A. Distinct localization and modulation of Cav1.2 and Cav1.3 L-type Ca^{2+} channels in mouse sinoatrial node. *J Physiol* 2012;**590**:6327–6342.
11. Neco P, Torrente AG, Mesirca P, Zorio E, Liu N, Priori SG, Napolitano C, Richard S, Benitah JP, Mangoni ME, Gomez AM. Paradoxical effect of increased diastolic Ca^{2+} release and decreased sinoatrial node activity in a mouse model of catecholaminergic polymorphic ventricular tachycardia. *Circulation* 2012;**126**:392–401.
12. Qu Y, Baroudi G, Yue Y, Boutjdir M. Novel molecular mechanism involving alpha1D (Cav1.3) L-type calcium channel in autoimmune-associated sinus bradycardia. *Circulation* 2005;**111**:3034–3041.
13. Hund TJ, Mohler PJ. Ankyrin-based targeting pathway regulates human sinoatrial node automaticity. *Channels (Austin)* 2008;**2**:404–406.
14. Mesirca P, Alig J, Torrente AG, Muller JC, Marger L, Rollin A, Marquilly C, Vincent A, Dubel S, Bidaud I, Fernandez A, Seniuk A, Engeland B, Singh J, Miquerol L, Ehmke H, Eschenhagen T, Nargeot J, Wickman K, Isbrandt D, Mangoni ME. Cardiac arrhythmia induced by genetic silencing of 'funny' (f) channels is rescued by GIRK4 inactivation. *Nat Commun* 2014;**5**:4664.
15. Chen B, Wu Y, Mohler PJ, Anderson ME, Song LS. Local control of Ca^{2+}-induced Ca^{2+} release in mouse sinoatrial node cells. *J Mol Cell Cardiol* 2009;**47**:706–715.
16. Bogdanov KY, Vinogradova TM, Lakatta EG. Sinoatrial nodal cell ryanodine receptor and Na(+)-Ca(2+) exchanger: molecular partners in pacemaker regulation. *Circ Res* 2001;**88**:1254–1258.
17. van Borren MM, Verkerk AO, Wilders R, Hajji N, Zegers JG, Bourier J, Tan HL, Verheijck EE, Peters SL, Alewijnse AE, Ravesloot JH. Effects of muscarinic receptor stimulation on Ca^{2+} transient, cAMP production and pacemaker frequency of rabbit sinoatrial node cells. *Basic Res Cardiol* 2010;**105**:73–87.
18. Joung B, Zhang H, Shinohara T, Maruyama M, Han S, Kim D, Choi EK, On YK, Lin SF, Chen PS. Delayed afterdepolarization in intact canine sinoatrial node as a novel mechanism for atrial arrhythmia. *J Cardiovasc Electrophysiol* 2011;**22**:448–454.
19. Copello JA, Zima AV, Diaz-Sylvester PL, Fill M, Blatter LA. Ca^{2+} entry-independent effects of L-type Ca^{2+} channel modulators on Ca^{2+} sparks in ventricular myocytes. *Am J Physiol Cell Physiol* 2007;**292**:C2129–C2140.
20. Satoh H, Katoh H, Velez P, Fill M, Bers DM. Bay K 8644 increases resting Ca^{2+} spark frequency in ferret ventricular myocytes independent of Ca influx: contrast with caffeine and ryanodine effects. *Circ Res* 1998;**83**:1192–1204.

21. Trafford AW, Sibbring GC, Diaz ME, Eisner DA. The effects of low concentrations of caffeine on spontaneous Ca release in isolated rat ventricular myocytes. *Cell Calcium* 2000;**28**:269–276.

22. Eisner DA, Choi HS, Diaz ME, O'Neill SC, Trafford AW. Integrative analysis of calcium cycling in cardiac muscle. *Circ Res* 2000;**87**:1087–1094.

23. Greensmith DJ, Galli GL, Trafford AW, Eisner DA. Direct measurements of SR free Ca reveal the mechanism underlying the transient effects of RyR potentiation under physiological conditions. *Cardiovasc Res* 2014;**103**:554–563.

24. Hua R, Adamczyk A, Robbins C, Ray G, Rose RA. Distinct patterns of constitutive phosphodiesterase activity in mouse sinoatrial node and atrial myocardium. *PLoS One* 2012;**7**:e47652.

25. Vinogradova TM, Sirenko S, Lyashkov AE, Younes A, Li Y, Zhu W, Yang D, Ruknudin AM, Spurgeon H, Lakatta EG. Constitutive phosphodiesterase activity restricts spontaneous beating rate of cardiac pacemaker cells by suppressing local Ca^{2+} releases. *Circ Res* 2008;**102**:761–769.

26. Le Scouarnec S, Bhasin N, Vieyres C, Hund TJ, Cunha SR, Koval O, Marionneau C, Chen B, Wu Y, Demolombe S, Song LS, Le Marec H, Probst V, Schott JJ, Anderson ME, Mohler PJ. Dysfunction in ankyrin-B-dependent ion channel and transporter targeting causes human sinus node disease. *Proc Natl Acad Sci USA* 2008;**105**:15617–15622.

27. Masson-Pevet M, Bleeker WK, Gros D. The plasma membrane of leading pacemaker cells in the rabbit sinus node. A qualitative and quantitative ultrastructural analysis. *Circ Res* 1979;**45**:621–629.

28. Valdivia HH, Kaplan JH, Ellis-Davies GC, Lederer WJ. Rapid adaptation of cardiac ryanodine receptors: modulation by Mg^{2+} and phosphorylation. *Science* 1995;**267**:1997–2000.

29. Vinogradova TM, Bogdanov KY, Lakatta EG. β-Adrenergic stimulation modulates ryanodine receptor Ca(2+) release during diastolic depolarization to accelerate pacemaker activity in rabbit sinoatrial nodal cells. *Circ Res* 2002;**90**:73–79.

30. Song LS, Wang SQ, Xiao RP, Spurgeon H, Lakatta EG, Cheng H. β-Adrenergic stimulation synchronizes intracellular Ca(2+) release during excitation-contraction coupling in cardiac myocytes. *Circ Res* 2001;**88**:794–801.

31. Sah R, Ramirez RJ, Backx PH. Modulation of Ca(2+) release in cardiac myocytes by changes in repolarization rate: role of phase-1 action potential repolarization in excitation-contraction coupling. *Circ Res* 2002;**90**:165–173.

32. Zhou P, Zhao YT, Guo YB, Xu SM, Bai SH, Lakatta EG, Cheng H, Hao XM, Wang SQ. Beta-adrenergic signaling accelerates and synchronizes cardiac ryanodine receptor response to a single L-type Ca^{2+} channel. *Proc Natl Acad Sci USA* 2009;**106**:18028–18033.

33. Younes A, Lyashkov AE, Graham D, Sheydina A, Volkova MV, Mitsak M, Vinogradova TM, Lukyanenko YO, Li Y, Ruknudin AM, Boheler KR, Eyk JV, Lakatta EG. Ca^{2+}-stimulated basal adenylyl cyclase activity localization in membrane lipid microdomains of cardiac sinoatrial nodal pacemaker cells. *J Biol Chem* 2008;**283**:14461–14468.

34. Gao Z, Singh MV, Hall DD, Koval OM, Luczak ED, Joiner ML, Chen B, Wu Y, Chaudhary AK, Martins JB, Hund TJ, Mohler PJ, Song LS, Anderson ME. Catecholamine-independent heart rate increases require Ca^{2+}/calmodulin-dependent protein kinase II. *Circ Arrhythm Electrophysiol* 2011;**4**:379–387.

35. Kim JJ, Yang L, Lin B, Zhu X, Sun B, Kaplan AD, Bett GC, Rasmusson RL, London B, Salama G. Mechanism of automaticity in cardiomyocytes derived from human induced pluripotent stem cells. *J Mol Cell Cardiol* 2015;**81**:81–93.